Publication XIII

Lasse Aaltonen, Mikko Saukoski, and Kari Halonen. 2005. Fully integrated charge pump for high voltage excitation of a bulk micromachined gyroscope. In: Proceedings of the 2005 IEEE International Symposium on Circuits and Systems (ISCAS 2005). Kobe, Japan. 23-26 May 2005. Pages 5381-5384. ISBN 0-7803-8834-8.

Fully Integrated Charge Pump for High Voltage Excitation of a Bulk Micromachined Gyroscope

Lasse Aaltonen, Mikko Saukoski, Kari Halonen
Electronic Circuit Design Laboratory
Helsinki University of Technology
Espoo, Finland

***Abstract*—This paper describes a fully integrated excitation electronics, which enables quick start-up or powerful continuous stage drive of a resonating sensor. The system of a micromechanical resonator, readout circuitry and high voltage drive electronics is connected to form a positive feedback from the capacitive readout of the sensor to the drive electrodes. The charge pump circuit converts the low voltage signal at the resonant frequency to a 20 V differential square wave. The functionality is verified by forming a positive feedback loop and measuring the start-up time of a bulk micromechanical gyroscope. Measured charge pump is implemented within chip area of 0.46 mm^2 and draws 0.9 mA from a 5 V supply.**

I. INTRODUCTION

Micromechanical sensors with fully integrated interface electronics have enabled the vast use of low-cost micro-electro-mechanical systems (MEMS). One of the major targets for low cost sensors is the automotive industry, which requires a variety of sensors for different applications. From the automotive solution point of view, especially when gyroscopes are considered, one of the important features is the sensor start-up time, the time it takes the system to be operational after the power is switched on. Gyroscopes can be used for example for vehicle chassis control.

In the operational mode, relatively much energy is stored in bulk micromachined gyroscope's resonator. Like bulk micromechanical resonating sensors in general the tested gyroscope requires powerful drive signal to rapidly transfer the required energy to the resonator. A micromechanical resonator can be excited by using capacitive coupling. The force applied to the mechanical element is calculated as negative gradient of the interconnect capacitance energy,

$$\overline{F} = -\frac{\partial E}{\partial x}\overline{u_x} = -\frac{\partial C_{\text{int}} U^2}{2\partial x}\overline{u_x}, \qquad (1)$$

where U is the applied voltage and x is the displacement in the direction of x-axis. The size of the capacitor C_{int} can be calculated from the geometry of the sensor. The voltage U has both dc and ac component

$$U = U_{DC} + U_{AC}\sin(\omega_0 t), \qquad (2)$$

where ac component is at the resonance frequency ω_0. By combining (1) and (2) the force at the resonance frequency is given approximately as

$$\overline{F_{x\omega_0}} \approx \psi U_{DC} U_{AC}\sin(\omega_0 t)\overline{u_x}, \qquad (3)$$

where ψ is a constant dependent on sensor geometry. According to (3) to excite the resonator at resonance frequency both dc and ac voltage components are required.

II. POSITIVE FEEDBACK

The positive feedback is formed by reading the change in sensor capacitance and connecting the voltage mode signal amplified and 90 degrees phase shifted to the sensor excitation electrodes. The block diagram is presented in Fig. 1. The first block in the readout chain is a charge sensitive amplifier followed by a high pass and a low pass filter. Phase shift is implemented with a derivator. After phase shifting, the signal is converted to square wave with a comparator, which controls the charge pump. Charge pump generates differential 20 V square wave to the excitation electrodes of the sensor.

The 90 degree phase shift between the read signal and excitation voltage is desired but due to numerous non-idealities there is always some phase error present. In this case the phase shift in the chain will be $90^\circ + \varphi_{err}$. The effect of the phase error to the oscillation amplitude and power can

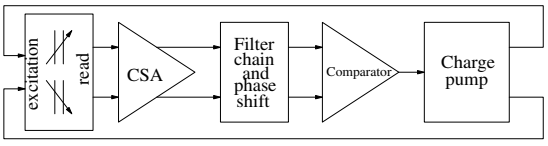

Figure 1. Block diagram of the sensor excitation system.

The project under which this work was done is funded by National Technology Agency of Finland (TEKES) and VTI Technologies Oy. The Design tools were provided by Cadence Design Systems and Mentor Graphics.

be evaluated by dividing the excitation voltage into in-phase and out-of-phase quadrature components. The quadrature component has the same phase as the resonator mass movement and will thus deliver no energy to the sensor. Due to the high Q-value of the sensor, the square wave drive signal can be considered as sinusoidal with the same frequency as the fundamental frequency of the square wave. Thus by assuming that the power is transferred at the fundamental frequency and in correct phase we can write for the drive signal

$$D\sin(\omega_0 t + \varphi_{err}) = B\sin(\omega_0 t) + C\cos(\omega_0 t)\,, \qquad (4)$$

where loop will have exactly 90 degrees phase shift if phase error φ_{err} is zero. Otherwise phase error will cause attenuation (B/D) of $\cos(\varphi_{err})$. This result indicates that small phase errors have negligible effect on resonator beam vibration amplitude. The amplitude C of the quadrature component can be neglected.

III. Charge Pump

Considering the chip area one of the most effective ways of creating voltages higher than the supply are voltage doublers [1]. However, as the drive voltages must be above 20 V, the transistors, which are used as switches, often cannot tolerate full scale gate-source voltages. This would lead to very complex clock generating circuits and start-up problems if doublers were used.

To avoid aforementioned problems traditional Dickson-type charge pumps with diodes can be used. When designing a fully integrated structure the traditional architecture developed by Dickson [2] with output voltage given as

$$V_{cp} = (N+1)(V_{Supply} - V_d)\,, \qquad (5)$$

can result in many stages N if the desired output voltage V_{cp} is much higher than the supply voltage V_{Supply} reduced by a diode drop V_d. The equation excludes the effect of stray capacitances and assumes zero resistive load. In order to optimize the output voltage versus chip area, the voltage can be increased by two different pumps by using the first stage voltage for the generation of second stage clock signals. The block diagram of this kind of voltage boosting structure is shown in Fig. 2. The blocks CP1 and CP2 are basic Dickson-type pumps, where N denotes the number of diode stages in one pump. The blocks required for a second output are drawn in the picture with a dotted line. To be able to fully utilize the voltage Vmid at the output of the first stage one must boost the swing of the clock that is used to pump the voltage of the second stage. This can be easily done by using a cross coupled differential pair presented in Fig. 2. The circuit can be controlled by low voltage clock signals clk2 and xclk2 as long as their voltage level is high enough to turn the NMOS-transistors M3 and M4 on. In addition transistors M1 and M2 must be able to tolerate gate-source voltages as high as –Vmid. The medium voltage clock signals are then used as clocking signals for the second stage. If the supply voltage used is large enough the diode voltage drop can be

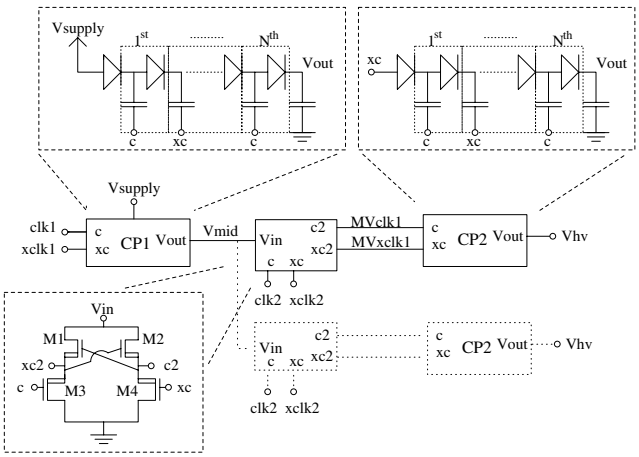

Figure 2. Block diagram of the presented two stage charge pump structure.

tolerated and Dickson charge pumps can be used in both stages of the pump. Voltage gain of the two stage pump of Fig. 2 is given as

$$V_{cp} = (N_2+1)(V_{mid} - V_d)\,. \qquad (6)$$

V_{mid} can be solved from equation

$$V_{mid} = N_1\left(V_{Supply} - V_d - xN_2V_{mid}\right) + \left(V_{Supply} - V_d\right), \quad (7)$$

where N_1 and N_2 denote the number of diode stages and

$$x = I_L/(CN_2f_1V_{mid}) = C_p f_2/(Cf_1)\,, \qquad (8)$$

where I_L is the load current drawn by the second stage, C the capacitance of one of the first pump stage capacitors, f_1 the first stage pumping frequency, C_p is the parasitic capacitance per capacitor at the second stage and f_2 the pumping frequency of the second stage. By substituting V_{mid} solved from (7) to (6) and assuming that $V_d \ll V_{mid}$ in (6) we get

$$\mathrm{V_{cp}} \approx (N_1+1)(N_2+1)\left(\frac{V_{Supply} - V_d}{1+N_1N_2x}\right),$$

which assumes zero load current of the second stage and that only the parasitic capacitances load the first stage.

A. Optimization

Let us define the unity area constant to be the relative chip area per one diode and one capacitor. For low voltages higher capacitor densities can be used and therefore first and second stage will have different constants y denoting the relative area. There is also the level shifter, an extra diode and a capacitor at the output of the first stage, which will have a small constant contribution to final area. The approximation of the relative chip area is thus given as

$$A(N_1, N_2) = N_1y_1 + N_2y_2 + y_3\,, \qquad (9)$$

where N_1 and N_2 are the number of diode stages in the first and second pump stage and y_1 and y_2 are the constants which define the relative size of a single diode stage of a pump. If we now solve N_2 from (6), substitute the result into (9) and differentiate the resulting equation and set the derivative to be zero we get the optimal number of diode stages in the first pump. Result is given as

$$N_1 = \sqrt{\frac{y_2}{y_1}\frac{V_{cp}}{V_{Supply}-V_d-xV_{cp}}} - \frac{V_{Supply}-V_d}{V_{Supply}-V_d-xV_{cp}}. \quad (10)$$

The accurate evaluation of relative chip areas consumed by the charge pumps is very difficult. Rough evaluation of the required N_1 can be obtained by setting constants y_1 and y_2 equal. This enables bigger capacitance in the first stage to compensate for second stage parasitics. For the designed structure V_{cp} was required to be at minimum 20 V, supply is 5 V, diode drop is 0.66V and constant x is 0.015. Using (10) we get the results N_1 equa1s 1 and N_2 2. Number of diode stages in a single stage pump implementation is 5. The difference between the number of diode stages will become more noteworthy with low supply voltages. Instead of area optimization more usually the output voltage of the first stage is limited by some other constraint such as the gate-source voltage of the level shifter PMOS-transistor or voltage limitation of the first stage capacitors. When two simultaneously used outputs are required, the second stage needs to be doubled and the constants y_2 and A must be multiplied by two for correct optimization.

The second stage of the implemented charge pump is presented in Fig. 3. This stage with clock signal level shifter is doubled in order to generate two independent high voltage square waves. Fig. 3 also shows the switches that control the high voltage output Vhv. The usage of floating switches would have resulted in difficult control signal generation because transistors cannot tolerate full scale gate-source voltages. This is avoided by the use of non-floating switches and by resetting the whole second stage when zero voltage output is required. This is done by turning clock signals clk2 and xclk2 of the level shifter in Fig. 2 off and both transistors M1 and M2 of Fig. 3 on. As the medium voltage clock signal node MVxclk1 stays low and MVclk1 high, no current will flow through M1 or M2 in continuous state. The pump structure presented in Fig. 3 also enables a high impedance output mode, when M2 is off and M1 on. This way, after the quick start-up of the resonating sensor is performed, the pump can be turned completely off and continuous mode excitation of the sensor can be performed with accurately controlled low voltage signal.

B. The Effect of Charge Pump Output Impedance

The effective output impedance of the pump will define the maximum switching speed of Vhv. Due to the large impedance of the charge pump the rise time of the output square wave will be quite long. The fall time will be short, because the voltage is reset with a switch. Fourier series will show the effect of slow rise time to the amplitude of the component at the fundamental frequency. For the periodic waveform of Fig. 4 the Fourier coefficients are calculated as

$$a_n = \frac{2}{T}V_0 \int_0^{T/2} (1-e^{-t/\tau}) \sin(n\omega t)dt\,, \quad (11)$$

where V_0 is the maximum output voltage of the charge pump, T is the period and ω is the angular frequency of the square wave. At the fundamental frequency, we get

$$a_1 = \frac{2V_0}{\pi}\left[1 - \frac{2\pi^2}{(T/\tau)^2 + 4\pi^2}(1+e^{-T/(2\tau)})\right], \quad (12)$$

where the time constant τ is formed by the load capacitor and the effective output impedance of the charge pump. If the sine function is replaced with cosine function in (11), the resulting quadrature component has no effect on sensor energy. The attenuating effect of rise time given by equation (12) is 9.1 % when comparing fundamental component amplitudes with zero rise time and when T/τ is 10.

C. Clocking of the Charge Pump

To be able to use the charge pump structure described above the clock frequency must be about two decades higher than the frequency of the square wave. The medium voltage Vmid clock can have lower frequency than the first stage clock signals. This will considerably lower the component sizes at the first Dickson-type charge pump stage. The implemented clock generator has the second stage clock frequency divided by four. Size of the charge pump load capacitor will have effect on the required clock frequency. Accurate clocking frequency is not required as the level of high voltage signals would still have temperature and process dependency. In addition, phase noise properties are of no importance. Clock frequency must however be adequate to obtain high enough worst case voltage.

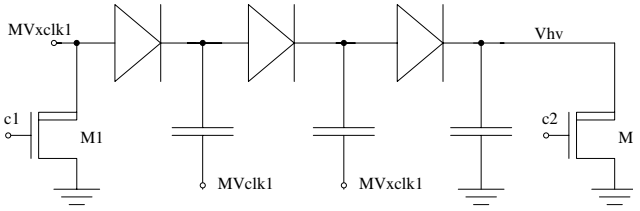

Figure 3. The second part of the charge pump.

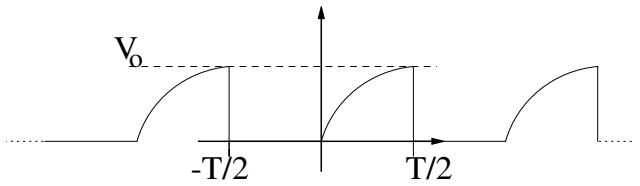

Figure 4. High voltage signal waveform.

IV. MEASUREMENTS

The excitation loop was implemented with a 0.7 μm double-metal, double-poly high voltage BiCMOS process that offers high-ohmic polysilicon resistors, good-quality analog capacitors and floating diodes. The micrograph of the circuit is shown in Fig. 5. The chip area consumed by the pump is 0.46 mm^2. The used supply voltage is 5 V and the current consumption of the charge pump is 0.9 mA in the operational mode. The resonator which was used for testing the excitation electronics was a bulk micromachined gyroscope. The SEM picture of the sensor is in Fig. 5.

The functionality of the charge pump was tested by applying input signal directly to the comparator. The pump response to a 5 kilohertz signal is shown in Fig. 6. Figure shows both outputs, which form a differential high voltage square wave. Measurement shows that the system can be used at frequencies above 10 kilohertz before the signal component at the fundamental frequency, given by (12), is considerably attenuated. Unloaded DC output was measured to be 21.7 V. The result given by (6) is 23.3 V. The difference in voltages results from process variations and various parasitic resistors and capacitors.

The output impedance of the charge pump was measured by loading the amplifier resistively and measuring the steady state output voltage. The impedance was calculated to be 500 kΩ, low enough to tolerate leakage currents and to drive the micromechanical resonator at 10 kilohertz frequency. The sensor excitation was detected by measuring the amplified CSA output during the start-up. Reset signal of the charge pump is removed after the supply voltage is connected. After this the excitation loop is closed and mechanical element starts to vibrate with increasing amplitude. Measured signal at start-up is presented in Fig. 7. Loop is closed at time instant 0 s, after which signal amplitude increases. After 230 ms, the mechanical vibration amplitude has reached the desired level, the pump is shut down and amplitude is kept constant. The start-up times with charge-pump and supply voltage limited signals can be compared by examining the force applied to the sensor. The reference voltage of the sensor is 5 V. The DC-component of the pump signal is 10 V and the fundamental frequency component of the differential square wave is π/2*20 V. Respectively, the supply limited signal has DC level of 2.5 V and resonance frequency component of π/2*5 V. According to (3) the force applied by the charge-pump is eight times higher compared to the force excited by the supply limited start-up signals.

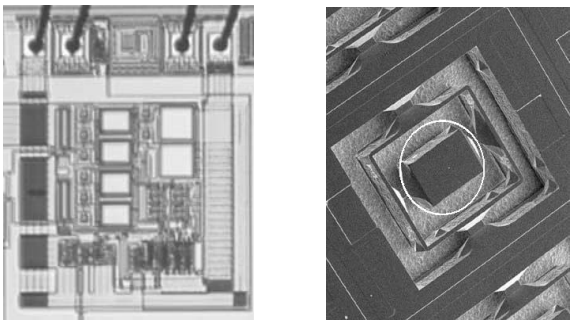

Figure 5. Left: Microphotograph of the implemented charge pump. Right: SEM picture of the gyroscope. Encapsulating wafers with electrodes are anodically bonded to both sides of the structural wafer. The excited resonator is encircled in the picture.

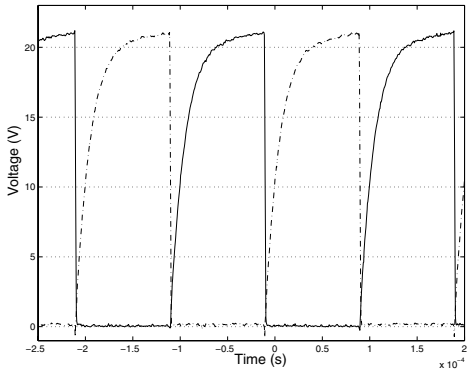

Figure 6. Measured charge-pump output waveforms at 5 kHz frequency.

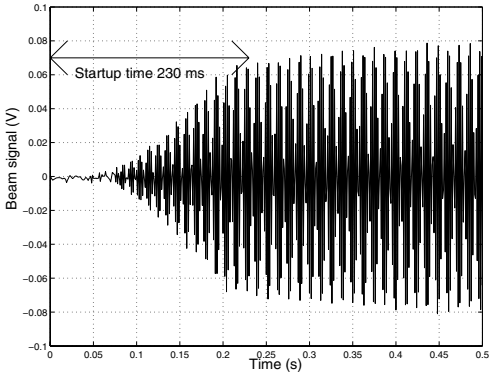

Figure 7. Measured gyroscope resonator signal during start-up. Signal is folded due to low sampling rate of the oscilloscope.

V. CONCLUSIONS

Fully integrated charge pump for the excitation of a resonating sensor was presented. The system was realized within chip area of 0.46 mm^2 and start-up of a bulk micromachined gyroscope was measured. The excitation force attained was eight times higher than that achieved by supply limited excitation. The measured results indicate that with small chip area contribution the drive of a micromechanical resonator can be boosted considerably.

ACKNOWLEDGEMENT

The authors wish to thank VTI Technologies Oy for providing the sensor elements.

REFERENCES

[1] Chi-Chang Wang and Jiin-chuan Wu. "Efficiency Improvement in Charge Pump Circuits" IEEE Journal of Solid-State Circuits, Vol. 32, No. 6, pp.852-860 June 1997.

[2] John F. Dickson. "On-Chip High-Voltage Generation in NMOS Integrated Circuits Using an Improved Voltage Multiplier Technigue." IEEE Journal of Solid-State Circuits, Vol. SC-11, No. 3, pp. 374-378, June 1976.